

Sand particle produced by unstable perforated wellbore

Ariffin Samsuri
Universiti Teknologi Malaysia, Kuala Lumpur, Malaysia



ABSTRACT: The paper presents the results of a laboratory study of the sand particle produced from unstable perforated wellbore. Section of a perforated wellbore were generated and expose to various loads and conclusions were drawn with respect to the produced sand particle during loading process, up to failure of the perforated wellbore structure. The results show that the perforated wellbore may fail during the creation process and sand particles were produced, depending on the perforated wellbore geometry or perforation parameters and rock properties. The sand particles produced were found by sieve analysis to be oversized 500 μ . Generally, stable perforated wellbore produced less sand particle, therefore minimizing the sand production problems.

1 INTRODUCTION

It is known that a reservoir rock is in equilibrium between overburden and pore fluid stresses, and in a triaxially stressed state. When perforations are created in the productive zone, rearrangement of the stress takes place and the surrounding rock must carry the redistributed load. This produces a stress concentration around the perforation tunnel, with maximum on the perforation wall which is correspond to Jaeger's conclusion on a hollow cylinder (Jaeger et al. (1979) and Obert et al. (1967)). The stress may exceed the peak strength of the rock and if the rock structure is not strong enough, the surrounding rock will fail and causing failure within the rock. This process may produce crushed material on the perforation face or the perforated wellbore may totally collapse, causing a reduction in well productivity or sand particle production.

Movement of sand particles into the wellbore as fluid is produced, is undoubtedly the primary production problem, which are most common in younger Tertiary sediments, particularly of the Miocene epoch. However, sand or rock failure can occur in other formation when local earth stress rates and rock strength are affected by certain drilling, completion practices and production operations that create an unstable condition, such as perforating. The sand particle production mechanism is exceedingly complex and it is influenced by every completion operation from first bit penetration to production period of the well. Sand particle production has become a major problem in many regions of the world. A high percentage of current exploration and development effort is being expended in these areas. Sand control is not only time-consuming and expensive, but also generally causes severe productivity restriction.

Sand particle has a tendency to move toward a wellbore as

fluids move in the reservoir unless some action is taken to prevent the movement. Sand particle flow from the formation can create a potentially serious and costly problems, such as; production loss, failure of casing or liners, abrasion of equipment and, handling and disposal of produced sand particles. Successful sand control application requires that each step of the drilling, completion and production be designed and executed properly.

Many studies have been conducted on the sand production problems, on sand control and on sand arch stability, but little attention has been paid in the literature to the study of sand particle produced by the unstable perforated wellbore.

2 THE LABORATORY WORK

The laboratory work used two types of models; i.e. blocks and hollow cylinders, using six different types of rock: yellow well cemented sandstone (YH), red well cemented sandstone (RH), white well cemented sandstone (WH), white well cemented with carbonaceous layers sandstone (WHWR), red sandstone with well cemented grain and carbonaceous layers (RHWR) and yellow loosely cemented sandstone (YS). The compressive strength of the sample vary from 22 to 32 MN/sq.m.

2.1 Block Models

The block models were prepared from sandstone rock samples by drilling a 127 mm diameter hole and were then trim into the desired size, i.e. 457 mm by 305 mm by 305 mm; . To represent the casing, a steel pipe of 102 mm inside diameter and 114 mm outside diameter was cut to the

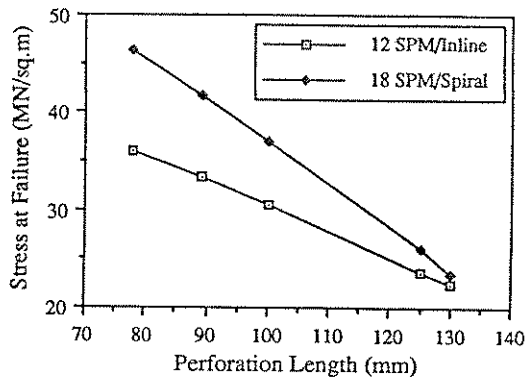


Fig. 1 Effect of Perforation Length on Perforated Wellbore Stability

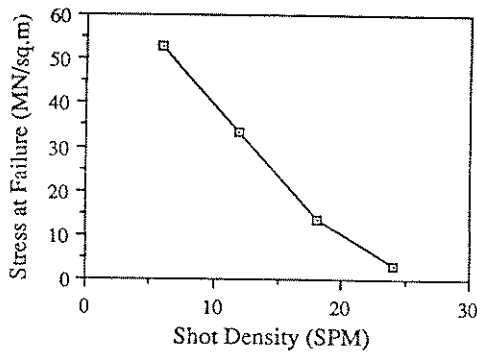


Fig. 2 Effect of Shot Density On Perforated Wellbore Stability

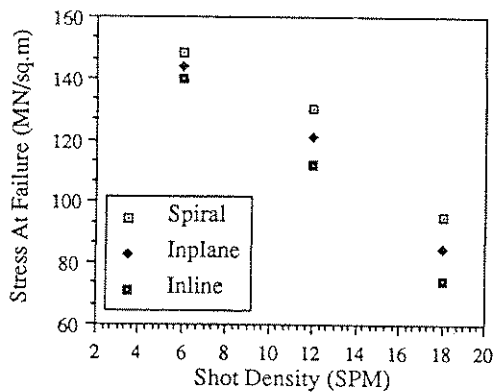


Fig. 3 Effect of Phasing and Pattern On Perforated Wellbore Stability

correct length. Once the steel pipes were of the correct dimension, the perforations were then drilled through the wall in accordance with the particular shot density, phasing angle, spacing and pattern of the block to be cemented, i.e. shot densities of 6, 12 and 18 shots per meter (SPM), diameter of 12 mm, phasing angle of 0, 60 and 90°, and inline, inplane and spiral pattern, by using 12 mm diameter bit. The perforated steel pipe was then cemented to the corresponding block using Fondu cement with 3 to 1 cement water ratio. The cemented block was left over for 24 hours to allow the cement to set. The perforations were then drilled right through the cement into the sandstone block to the desired depth; i.e. 78 to 130 mm, using 12 mm bit.

The blocks were then tested under uniaxial compression within a servo-controlled stiff testing machine at constant rate of 0.7 MN/sq.m/s until failure. A plot of axial load against axial deformation was produced to indicate the onset of failure of the block. After failure, any sand particles produced were then collected for sieve analysis.

2.2 Cylindrical Models

The cylindrical models of 55 mm diameter were cored from the sandstone rock samples. After coring, the specimens were then cut to the 110 mm length and the 28 mm diameter hole was then cored along the centre of the specimen with a 25 mm diameter bit. The perforations were then drilled into the annulus of rock left. Various shot densities, phasing and patterns, i.e. shot densities of 6, 12 and 18 SPM, perforation length of 13.5 mm, phasing angle of 0, 60 and 90°, and inline, inplane and spiral perforation patterns have been studied.

The cylindrical specimens were confined in a triaxial cell which was located within a servo-controlled stiff testing machine. A hollow cylindrical platen was produced and used at the bottom of the assembly through which the produced sand particles during loading process were collected. The cylindrical models were tested to failure at different confining pressure of 50, 100 and 150 bar. After failure which was indicated by sharp drop in load against displacement plot, any sand particles produced were brushed off and collected in a plastic sealable bag for sieve analysis.

2.3 Sieve Analysis Procedure

The sand particles produced by failure were weighed before being sieved, which was recorded as the recovered weight. The laboratory disc was then carefully emptied on the nested sieves. The sieve column was closed off with a cover to avoid contamination by dust or loss of sand particles. The nested sieve column was then shaken for 10 minutes using an electric sieve shaker ((Vicker (1978), Craig (1978) and Wills (1979)). After 10 minutes, the contents of each sieve was carefully brush off and then weighed. Consequently, the weight for each particle size range as defined by the mesh size range of successive sieves was calculated. The

amount of oversized and under-sized particles were then calculated. Cumulative percentage finer as cumulative percent finer on standard sieve sizes. The cumulative percentage of particle

3 RESULTS AND DISCUSSION

In general, the results show that the perforated wellbore stability and sand particles produced during failure depend on the perforation phasing angle and pattern, and perforation length. The produced sand particles are characterized by the gross deformation and stress at failure. The big portion of sand particles is finer than 500µ, ranging from 27% to 35%. More stable perforated wellbore stability is observed. The sand particle created within the perforation tunnel surface will be collected during the production in the wellbore.

3.1 Perforated Wellbore Stability

Fig. 1 shows that 12 SPM, inline perforations length of 89 mm fail at 36 MN/sq.m while the perforations 125 mm fail at 23.61 MN/sq.m. This shows that wellbore stability decreases as perforation length increases. Fig. 1 also shows that the perforation pattern with 79 mm perforation length fails at 46 MN/sq.m, while the perforations fail at 24 MN/sq.m. This shows that the perforation length effect on wellbore stability also depends on shot density and perforation pattern.

The 18 SPM, inline perforation with 125 mm length fails at 26 MN/sq.m stress; i.e. fails at 14 MN/sq.m stress; i.e. fails at 14 MN/sq.m stress. The results show that perforated wellbore stability increases even as the shot density increases. Increasing shot density reduces the amount of rock matrix that must be carried for more load must be carried for more load must be carried resulting in reduction of rock matrix.

By changing the phasing angle from 0 to 90° and the pattern from inline to spiral, the spiral pattern fails at higher stress than the inline pattern. This figure also shows that an inline pattern fails at lower stress than the spiral inline pattern. In general, the results show that the perforation phasing angle with spiral pattern is more stable than an inplane pattern, and

steel pipes were of the correct size were then drilled through the sandstone block to be cemented, i.e. 18 shots per meter (SPM), phasing angle of 0, 60 and 90°, and pattern, by using 12 mm diameter pipe was then cemented to the concrete with 3 to 1 cement sand. The block was left over for 24 hours before the perforations were then drilled into the sandstone block to the 30 mm, using 12 mm bit. The specimens were tested under uniaxial compression on a stiff testing machine at constant load until failure. A plot of axial load versus displacement was produced to indicate the onset of failure, any sand particles produced were collected for sieve analysis.

5 mm diameter were cored from the specimens. After coring, the specimens were cut to the required length and the 28 mm diameter hole was drilled through the center of the specimen with a 12 mm diameter bit. The specimens were then drilled into the sandstone block at various shot densities, phasing and phasing angle of 0, 60 and 90°, and perforation patterns have been used.

The specimens were confined in a triaxial cell and tested on a servo-controlled stiff testing machine. The specimens were tested under uniaxial compression on a stiff testing machine at constant load until failure. A plot of axial load versus displacement was produced to indicate the onset of failure, any sand particles produced were collected for sieve analysis.

The specimens were tested under uniaxial compression on a stiff testing machine at constant load until failure. A plot of axial load versus displacement was produced to indicate the onset of failure, any sand particles produced were collected for sieve analysis.

amount of oversized and undersized sand particles were then calculated. Cumulative percentage oversized is defined as cumulative percentage of particle retained on the sieves. The cumulative percentage undersized is the cumulative percentage of particle passing through these sieves.

3 RESULTS AND DISCUSSION

In general, the results show that the perforated wellbore may fail and sand particles were produced. The perforated wellbore stability, sand particles produced and the particle size distribution depend on the perforation length, shot density, phasing angle and pattern, and rock properties, as summarized in Table 1. The produced sand particles were related to the gross deformation and stability of the perforated wellbore. The big portion of sand particles produced are larger than 500µ, ranging from 27 % to 88 % of recovered weight. More stable perforated wellbore produce less sand particle. The sand particle created within the rock adjacent the perforation tunnel surface will contribute to any sand production in the wellbore.

3.1 Perforated Wellbore Stability

Fig. 1 shows that 12 SPM, inline perforation pattern with perforations length of 89 mm fail at 33.33 MN/sq.m stress, while the perforations 125 mm in length fail at a lower stress, equal to 23.61 MN/sq.m. This indicates that the perforated wellbore stability decreases as the perforation length increases. Fig. 1 also shows that 18 SPM, 60° phasing spiral perforation pattern with 79 mm length appears to fail at a stress equal to 46 MN/sq.m, while the 130 mm length perforations fail at 24 MN/sq.m. stress. The results show that the perforation length effect on the perforated wellbore stability also depends on shot density, phasing angle and pattern.

The 18 SPM, inline perforation with 79 mm length fails at 14 MN/sq.m. stress; i.e. fails at lower stress than the 12 SPM perforation with 89 mm length, as shown in Fig. 2. These results show that perforated wellbore stability decreases as the shot density increases even though the perforation length decreases. Increasing shot densities by definition reduce the amount of rock matrix within the system, therefore more load must be carried by the surrounding rock, resulting in reduction of rock mass strength. These results also show that the shot density effect is more dominant than the perforation length.

By changing the phasing angle of 12 SPM perforation from 0 to 90° and the pattern from inline to spiral, the results show that the spiral pattern fails at higher stress, as shown in Fig. 3. This figure also shows that an inplane perforation pattern fails at lower stress than the spiral pattern but higher than the inline pattern. In general, the results show that increasing the perforation phasing angle will increase stability, depending on the perforation pattern: the spiral pattern is more stable than an inplane pattern, and both are more stable than

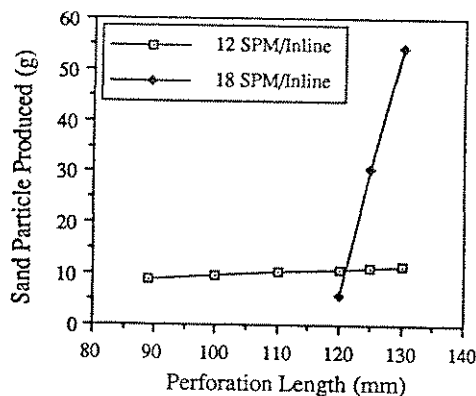


Fig. 4 Effect of Perforation Length On Sand Particles Produced

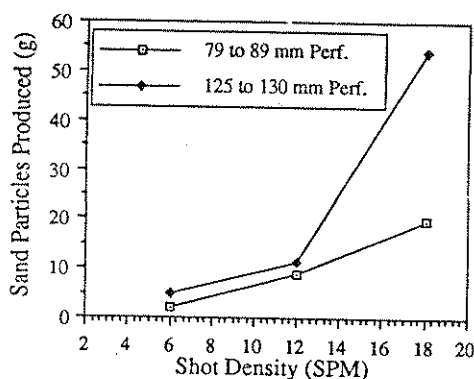


Fig. 5 Effect of Shot Density On Sand Particles Produced

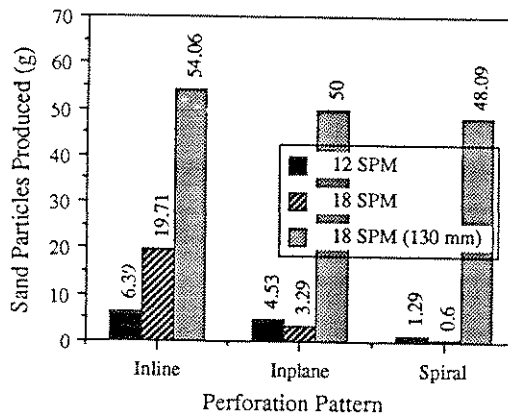


Fig. 6 Effect of Phasing Angle And Pattern On Sand Particles Produced

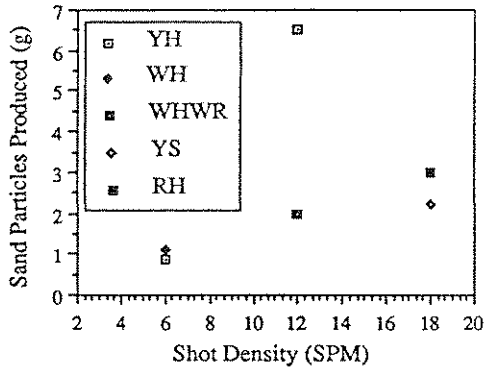


Fig. 7 Effect of Rock Type On Sand Particles Produced

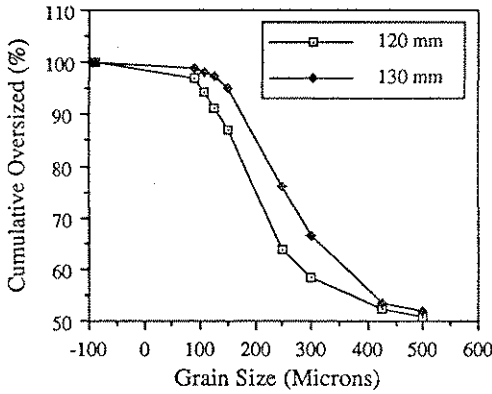


Fig. 8 Effect of Perforation Length On Sand Particles Size Distribution

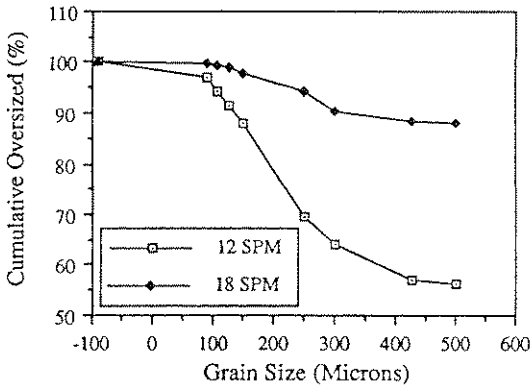


Fig. 9 Effect of Shot Density On Sand Particles Size Distribution

an inline pattern. This is because in the spiral perforation pattern, the perforation tunnels are in a plane inclined to the direction of applied stress (major stress), therefore the strength of the rock mass is higher than for the inplane pattern where the perforation tunnels are in one horizontal line perpendicular to the major stress, resulting in lower rock mass strength. On the other hand, in an inline perforation pattern, the perforation tunnels are in a line parallel to the major stress, resulting in the lowest rock mass strength.

It is evident that rock type is an important factor to the perforated wellbore stability; the stability increases as the strength of rock increases; since the rock becomes stronger and has greater ductility. The experimental results show that 6 SPM, spiral perforation in the YH sandstone fails at higher stress (125 MN/sq.m) than in the WH sandstone, which fails at 72 MN/sq.m. And, 6 SPM, inplane perforation in the RH sandstone fails at higher stress (109 MN/sq.m) than in the WH sandstone which fails at 75 MN/sq.m. However, 18 SPM, inplane perforations in the YH sandstone fail at 109 MN/sq.m, while in the RH sandstone, it fails at 74 MN/sq.m. In addition, 12 SPM, spiral perforations in the YH sandstone fails at 130 MN/sq.m, while in the WHWR sandstone, it fails at 81 MN/sq.m. And, 18 SPM, spiral perforation in the RH sandstone fails at 94 MN/sq.m, but fails at 51 MN/sq.m in the YS sandstone. From the above results, it is clear that the perforated wellbore in the YH sandstone is more stable than in the RH sandstone, and both are more stable than in the WH sandstone. On the other hand, the perforated wellbore in the WH sandstone is more stable than in the WHWR sandstone, and both are more stable than in the YS sandstone.

3.2 Sand Particle Produced

Increasing 12 SPM, inline perforation length from 89 mm to 125 mm will increase sand particles produced at failure from 9 g to 11 g, or 40 % increase in length will increase the particles by 30 %, as shown in Fig. 4. This result shows that the sand particle produced at failure increases as the perforation length increases. Fig. 4 also shows that the effect becomes greater as the shot density increases, as shown by increasing the length of inline 18 SPM perforation from 120 mm to 130 mm will increase the sand produced from 6 g to 54 g.

Fig. 5 shows that increasing the shot density from 12 to 18 SPM will increase the sand particles produced from 9 g to 11 g for shorter length (78 mm to 89 mm) and from 11 g to 15 g for longer perforation length (125 mm to 130 mm). The results show that increasing in shot density will increase the sand particles produced by collapse perforated wellbore since the stability decreases. The overall results also show that the effect of shot density on the sand particles produced depends on perforation length, phasing and pattern, and rock strength.

The results as shown in Fig. 6 show that changing the phasing angle of 12 SPM perforation from 0 to 90° (which also changes the pattern from inline to inplane or spiral), will

decrease the sand particles produced. This is because in the spiral perforation pattern, the perforation tunnels are in a plane inclined to the direction of applied stress (major stress), therefore the strength of the rock mass is higher than for the inplane pattern where the perforation tunnels are in one horizontal line perpendicular to the major stress, resulting in lower rock mass strength. On the other hand, in an inline perforation pattern, the perforation tunnels are in a line parallel to the major stress, resulting in the lowest rock mass strength. It is evident that rock type is an important factor to the perforated wellbore stability; the stability increases as the strength of rock increases; since the rock becomes stronger and has greater ductility. The experimental results show that 6 SPM, spiral perforation in the YH sandstone fails at higher stress (125 MN/sq.m) than in the WH sandstone, which fails at 72 MN/sq.m. And, 6 SPM, inplane perforation in the RH sandstone fails at higher stress (109 MN/sq.m) than in the WH sandstone which fails at 75 MN/sq.m. However, 18 SPM, inplane perforations in the YH sandstone fail at 109 MN/sq.m, while in the RH sandstone, it fails at 74 MN/sq.m. In addition, 12 SPM, spiral perforations in the YH sandstone fails at 130 MN/sq.m, while in the WHWR sandstone, it fails at 81 MN/sq.m. And, 18 SPM, spiral perforation in the RH sandstone fails at 94 MN/sq.m, but fails at 51 MN/sq.m in the YS sandstone. From the above results, it is clear that the perforated wellbore in the YH sandstone is more stable than in the RH sandstone, and both are more stable than in the WH sandstone. On the other hand, the perforated wellbore in the WH sandstone is more stable than in the WHWR sandstone, and both are more stable than in the YS sandstone.

3.3 Sand Particles Size Distribution

The results in Fig. 8 shows that the sand particles produced as the perforation length increases. It also shows that increasing the perforation length from 120 mm to 130 mm will increase the sand particles produced from 6 g to 54 g. As shot density increases from 12 SPM to 18 SPM, the sand particles produced will increase from 9 g to 15 g. The effect of shot density increases, as shown by Fig. 5. A perforation length of 125 mm will increase the sand particles produced by 30 %, as shown in Fig. 4. This result shows that the sand particle produced at failure increases as the perforation length increases. These results show that increasing the larger sand particles produced as the perforation length increases.

Fig. 11 shows that changing the phasing angle from 0 to 60° will reduce the sand particles produced from 88 g to 54 g. The inplane and spiral pattern, respectively, show that 60° phasing with larger sand particles from the spiral pattern is the most stable.

Fig. 12 shows that the sand particles produced by the perforated wellbore depends on the rock type. The effect of shot density on the sand particles produced depends on perforation length, phasing and pattern. It shows that sand particles produced from spiral perforation will increase as the shot density increases, and oversized 500µ of sand

because in the spiral perforation wells are in a plane inclined to the stress (major stress), therefore the stress is higher than for the inplane perforation tunnels are in one horizontal major stress, resulting in lower stress; other hand, in an inline perforation tunnels are in a line parallel to the lowest rock mass strength. Shot density is an important factor to the stability: the stability increases as the shot density increases, since the rock becomes stronger. The experimental results show that in the YH sandstone fails at higher stress than in the WH sandstone, which fails at lower stress. Inplane perforation in the RH sandstone (109 MN/sq.m) than in the YH sandstone (75 MN/sq.m). However, 18 SPM in the YH sandstone fail at 109 MN/sq.m, it fails at 74 MN/sq.m. Inplane perforations in the YH sandstone fail at 109 MN/sq.m, it fails at 51 MN/sq.m. Inplane perforation in the RH sandstone, but fails at 51 MN/sq.m. From the above results, it is clear that the YH sandstone is more stable than the WH sandstone, and the RH sandstone is more stable than in the YH sandstone. The perforated wellbore is more stable than in the WHWR sandstone, and the YH sandstone is more stable than in the YS sandstone.

decrease the sand particles produced at failure, since the perforated wellbore stability increases. The effect of phasing angle and pattern on the sand particles produced also depends on perforation length, shot density and rock type. Zero degree phasing angle (inline) of 12 SPM perforation produces 6 g of sand particles at failure but 90° phasing with inplane pattern produces 5 g sand particles. On the other hand, the spiral pattern indicates less sand particles are produced; i.e. 1.29 g only. The effect becomes greater as the shot density increases, as shown by changing the phasing angle of 18 SPM perforation (79 mm length) from 0 to 60° with inplane pattern will decrease the produced sand particles from 20 g to 3 g. But, the effect of changing phasing angle and pattern on the sand particles produced at failure becomes less as the length increases, as shown by changing 0° of 18 SPM and 130 mm length perforation to 60° phasing with spiral pattern which reduces the produced sand particles from 54 g to 48 g only.

On the other hand, the strength of the rock mass depends on the type of the rock. Therefore, the sand particles produced at failure also depends on the type of rock, as shown in Fig. 7.

5.3 Sand Particles Size Distribution

The results in Fig. 8 shows that more oversized 500µ of sand particles are produced as the length increases. This figure also shows that increasing the 18 SPM, inline perforation length from 120 mm to 130 mm will increase the oversized 500µ of sand particles from 51 % to 69 %.

As shot density increases from 12 to 18 SPM with length ranges from 78 mm to 89 mm, the oversized 500µ of sand particles produced will increase from 56 % to 88 %, as shown by Fig. 9. The effect becomes smaller as the length increases, as shown by Fig. 10. These figures show that for a perforation length of 125 mm to 130 mm, increasing the shot density from 12 to 18 SPM, will increase the oversized 500µ of sand particles produced from 46 % to 69 %, which is less than for perforation length range of 78 mm to 89 mm. These results show that increasing the shot density will increase the larger sand particles produced, depending on the perforation length.

Fig. 11 shows that changing the phasing angle of 18 SPM from 0 to 60° will reduce the oversized 500 microns of sand particles produced from 88 % to 36 % and 31 % for inline, inplane and spiral pattern, respectively. These results also show that 60° phasing with spiral pattern produces lesser larger sand particles from another two basic patterns since the spiral pattern is the most stable perforated structure.

Fig. 12 shows that the grain size distribution of sand particles produced by the perforated wellbore also depend on the rock type. The effect of rock type on sand particle size distribution depends on perforation length, shot density, phasing and pattern. It shows that oversized 500µ of sand particles produced from spiral perforation in the YH sandstone will increase as the shot density increases. On the other hand, oversized 500µ of sand particles produced from 18

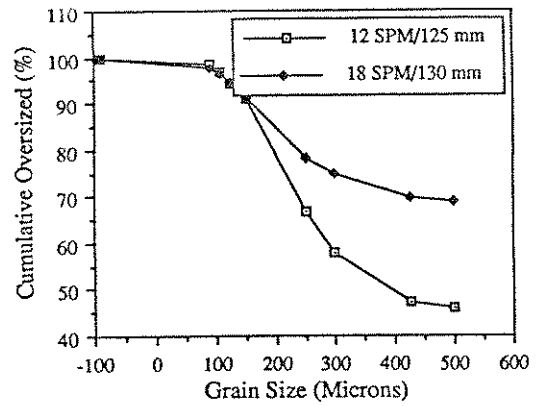


Fig. 10 Effect of Shot Density And Perforation Length On Sand Particles Size Distribution

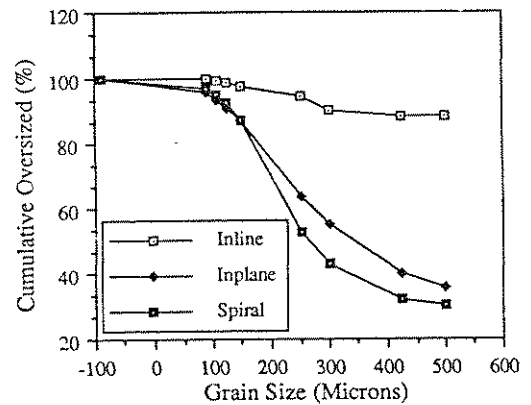


Fig. 11 Effect of Phasing Angle And Pattern On Sand Size Distribution

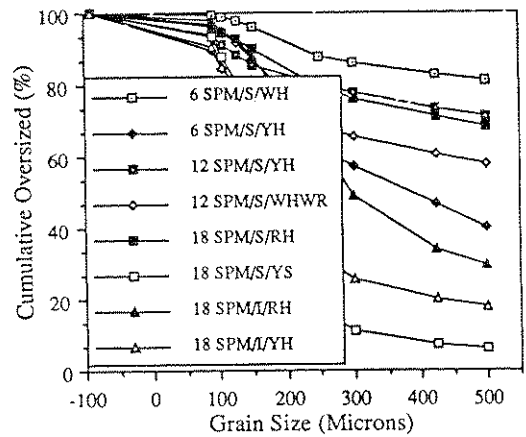


Fig. 12 Effect of Rock Type On Sand Particles Size Distribution

Table 1 : Summary of the Results

Factor Increased	Aspect		
	Perforated Wellbore Stability	Sand Particle Produced	Size Distribution (> 500 microns)
Perforation Length	Decrease	Increase	Increase
Shot Density	Decrease	Increase	Increase
Phasing Angle	Increase	Decrease	Decrease
Inline Pattern	Weakest	Highest	Highest
Inplane Pattern	Intermediate	Intermediate	Intermediate
Spiral Pattern	Strongest	Lowest	Lowest
Rock Strength	Increase	Increase	Decrease

SPM collapse perforations in the RH sandstone will increase as the pattern changes from inplane to spiral.

4 CONCLUSIONS

The study has shown that the perforated wellbore may fail and sand particles were produced, depending on the perforated wellbore geometry, such as perforation length, shot density, phasing angle, perforation pattern, and rock properties. The spiral pattern appears to be the most stable perforation pattern and the shot density effect is more dominant than the perforation length. Big portion of the sand particles produced were found by sieve analysis to be oversized 500 μ . The sand particles created within the perforated wellbore or the rock adjacent to the perforation tunnel surface will contribute to any sand production problems. Generally, stable perforated wellbore can minimize the sand particles production in the wellbore, therefore minimizing the sand production problems.

REFERENCES

- Craig, R.F, "Soil Mechanics", 2nd. edition, van Nostrand Reinhold Co., 1978.
- Jaeger, J.C. Cook & N.G.W, "Fundamental of Rock Mechanics" 3rd. edition, Chapman & Hall London, 1979.
- Obert, L & Duvall, W.I., "Rock Mechanics & The Design of Structure in Rock", John Wiley & Sons Inc., 1967.
- Vickers, B, "Laboratory Work In Civil Engineering" Granada Pub., London, 1978.
- Wills, B.B, "Mineral Processing Technology", Pergaman Press, Oxford, 1979.